Coexisting lattice contractions and expansions with decreasing thicknesses of Cu (100) nano-films

Simin An(安思敏)[1], Xingyu Gao(高兴誉)[1], Xian Zhang(张弦)[2], Xin Chen(陈欣)[1], Jiawei Xian(咸家伟)[1], Yu Liu(刘瑜)[1], Bo Sun(孙博)[1], Haifeng Liu(刘海风)[1], and Haifeng Song(宋海峰)[1,†]

[1] *Laboratory of Computational Physics, Institute of Applied Physics and Computational Mathematics, Beijing* 100088, *China*
[2] *Qian Xuesen Laboratory of Space Technology, China Academy of Space Technology, Beijing* 100094, *China*

(Received 11 February 2022; revised manuscript received 27 May 2022; accepted manuscript online 8 June 2022)

Lattice parameters are a basic quantity in material characterization, and a slight alteration in lattice parameters directly affects the properties of materials. However, there are still considerable controversies as to whether lattice expansion or contraction occurs in metallic nanomaterials with size reduction. Here, the size dependences of the lattice parameter and surface free energy of clean Cu (100) films are investigated via simulations. Lattice parameters of the exposed surfaces contract, whereas lattice expansion occurs along the direction perpendicular to the surfaces with decreasing film thicknesses. This is striking since the metallic bonds usually lack strong directionality, and it is always regarded that the lattice variations in all directions are consistent. The contraction parallel to the surface is more severe than the expansion perpendicular to the surface in films. The lattices change from cubic to tetragonal with decreasing film thickness. Consequently, common contractions and occasional expansions of the lattice parameters of Cu nanoparticles have been observed in previous experiments. Increasing free energy and surface free energy with decreasing thicknesses is the thermodynamic origin of the lattice variations. Our study therefore provides a comprehensive physical basis for the surface effects on the lattice variations.

Keywords: nanostructure, lattice variations, surface free energy, simulation

PACS: 68.55.–a, 64.60.an, 65.40.gp, 87.10.Tf **DOI:** 10.1088/1674-1056/ac76b5

1. Introduction

It is well known that a reduction in the size of nanomaterials causes anomalous changes in physical and chemical properties compared to their counterparts in bulk form.[1–5] One of the important applications of nanomaterials, such as nano-films and nanoparticles, is in the catalytic industry. In comparison to other metallic catalysts examined in electrokinetic experiments, copper (Cu) is the unique nonalloyed catalyst that is capable of realizing the efficient reduction of CO_2 into significant amounts of hydrocarbon products.[6,7] The selectivity of Cu films with (100), (110), and (111) facet orientation, respectively, favors the production of ethylene (C_2H_4), ethanol (C_2H_5OH), and ethylene (CH_4). It is inferred that Cu (100) is the dominant facet orientations of Cu polycrystal since the main production of Cu polycrystal is ethylene.[5,8] Extensive experiments have shown that the catalytical activity depends on the size of the electrode — the smaller, the better.[8–11] However, the underlying physical mechanism remains elusive until now.

The lattice parameter is a basic quantity in material characterization, and a slight alteration in lattice parameters directly affects the properties of materials. Although the size effects on lattice parameters have been frequently investigated for several decades, whether lattice contractions or expansions occur with decreasing material sizes is inconclusive until now.[12–14] An example of some of the most puzzling behavior is that both lattice contractions and expansions are experimentally reported in the same metal, like Ni, Pd, and Cu.[15–20] Since metallic bonds usually lack strong directionality, we may expect that lattice parameters in all directions contract or expand simultaneously when considering the nanoparticles in a liquid droplet model. However, metallic nanomaterials are quite different from liquids. In previous scientific research, the averaged lattice parameter is evaluated using XRD or ED, thus does not distinguish surface atoms from inner atoms. In comparison with nanoparticles, which are nano-sized in three dimensions, nano-films with one dimension in nanoscale are good at distinguishing the size effects on the surface from those effects on the interior.

Surface free energy is one of the fundamental thermodynamic parameters controlling a wide range of basic and applied phenomena.[21,22] The experimental observations of the size effects on catalytic behavior are believed to be correlated with the surface free energy.[5] Regrettably, the experimental measurements of surface free energy of crystalline metals are notoriously difficult, and experimental values of well-defined low-index orientations are practically unknown.[23,24] On the other hand, free energy cannot be determined directly from molecular dynamics simulations since neither free energy nor entropies can be expressed in terms of ensemble averages. The most applied indirect approach to compute free energy is the standard equilibrium thermodynamic integration method,

†Corresponding author. E-mail: song_haifeng@iapcm.ac.cn
© 2023 Chinese Physical Society and IOP Publishing Ltd

which computes the free-energy difference between the target system and a reference with known free energy by analyzing ensemble averages of the thermodynamic driving force for a sequence of constructed equilibrium states via a set of independent equilibrium simulations.[25–27] However, it is well known that this is hard and time-consuming work.[28,29] In recent years, nonequilibrium approaches relied on the rigorous theoretical basis of Jarzynski's equality[30,31] to bring new blood into the free energy calculation methods. The nonequilibrium thermodynamic integration method allows the calculations to be performed along an explicitly time-dependent process that can lead to significant efficiency gains without accuracy loss compared to standard equilibrium methods.[32,33] The continuous improvement of methods and the steady increase in computational power have substantially benefited the investigation of the thickness-dependent surface free energy of metals.

In this work, the thickness dependences of the lattice parameter and the surface free energy of clean Cu (100) films with a wide size ranging from ~ 0.5 nm to ~ 24 nm around room temperature were investigated using molecular dynamics simulations and the recently developed nonequilibrium thermodynamic integration method via the Large-scale Atomic/Molecular Massively Parallel Simulator (LAMMPS) packages.[32,34] We not only investigate the lattice parameter parallel to the surface, but also measure the lattice parameter perpendicular to the surface. Accordingly, we provide a reasonable explanation for the contradiction in lattice variations reported in previous literature. Furthermore, we establish a relationship between lattice variations and surface free energy, revealing the thermodynamic origin of lattice variations.

2. Methods

The films with top and bottom surfaces perpendicular to the z axis exposed in vacuum were created with 4, 7, 10, 13, 16, 19, 22, 25, 40, 55, 70, 85, and 130 atomic layers. Every atomic layer contained 320 atoms, as shown in Fig. 1. The cubic simulation box of Cu bulks contained 32000 atoms. The Cu atoms were modeled using the embedded-atom method (EAM) interatomic potential, which has been widely used to investigate the physical and chemical properties of Cu.[35–38] The simulation boxes were equilibrated at 200 K, 300 K, 400 K, and 0 GPa in the isothermal-isobaric ensemble (NPT) with a Nosé–Hoover thermostat and barostat before calculating their free energy. All the molecular dynamics (MD) simulations were performed using the LAMMPS packages.[34] For all simulations, periodic boundary conditions were applied in all three directions. The time step was chosen as 1 fs. The equations of motions were numerically integrated using the Verlet algorithm.

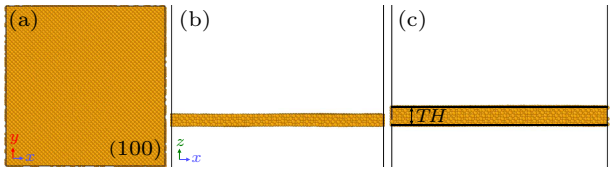


Fig. 1. The top (a) and side views [(b) and (c)] of the Cu films with (100) facet orientations.

The Helmholtz free energy of the films and bulks were computed using the nonequilibrium thermodynamic integration method: the Frenkel–Ladd path, which is described in detail in Ref. [32]. The Gibbs free energy of the films and bulks at $P = 0$ GPa is equal to the corresponding Helmholtz free energy. We employed the traversing Frenkel–Ladd thermodynamic path to calculate the free energy difference between the target system and the reference. The reference is chosen to be the widely used Einstein crystal, whose Hamiltonian can be expressed as

$$H_{\mathrm{E}} = \sum_{i=1}^{N} \left[\frac{p_i^2}{2m} + \frac{1}{2} m\omega^2 \left(r_i - r_i^0 \right)^2 \right]. \tag{1}$$

The free energy of an Einstein reference is written as

$$F_{\mathrm{E}}(N,V,T) = 3Nk_{\mathrm{B}}T \ln\left(\frac{\hbar\omega}{k_{\mathrm{B}}T} \right), \tag{2}$$

where k_{B} is the Boltzmann constant and $\hbar$ is the Planck's constant. All the atoms in an Einstein crystal perform a harmonic oscillator at the same lattice points as that in the target system. The oscillator frequency is obtained as $k = m\omega^2$, where the spring constant can be easily calculated from the mean-squared displacement $\langle (\Delta r)^2 \rangle$ as $k = 3k_{\mathrm{B}}T / \langle (\Delta r)^2 \rangle$. Thus, the free energy of an Einstein reference can be obtained analytically. The free energy difference ΔF between the target system and the reference E is calculated from the irreversible work between two states

$$w_{\mathrm{a}\to\mathrm{b}}^{\mathrm{irr}} = \int_0^{t_{\mathrm{s}}} \mathrm{d}t \left(\frac{\mathrm{d}\lambda}{\mathrm{d}t} \right) (H_{\mathrm{a}} - H_{\mathrm{b}})_{\Gamma(t)}. \tag{3}$$

In the nonequilibrium approach, the parametrical Hamiltonian H is set as

$$H(\lambda) = \lambda H_{\mathrm{E}} + (1-\lambda) H_0, \tag{4}$$

which is realized as the time-dependent parameter λ is varied from 0 to 1 in a switching time t_{s}, where $\lambda = \lambda(\tau) = \tau^5(70\tau^4 - 315\tau^3 + 540\tau^2 - 420\tau + 126)$. The Hamiltonian of the target system is

$$H_0 = \sum_{i=1}^{N} \frac{p_i^2}{2m} + U(\boldsymbol{r}), \tag{5}$$

where m is the mass of the atoms and $U(\boldsymbol{r})$ is the interatomic potential. Combining the forward and backward switching processes, the desired free energy difference can be estimated as

$$\Delta F = \int_0^1 \mathrm{d}\lambda \left\langle \frac{\partial H}{\partial \lambda} \right\rangle_{\lambda} = \frac{1}{2} (w_{0\to\mathrm{E}}^{\mathrm{irr}} - w_{\mathrm{E}\to 0}^{\mathrm{irr}}), \tag{6}$$

where $\langle \ldots \rangle_\lambda$ is the canonical ensemble average for a coupling parameter λ that is varied from 0 to 1. The free energy of the target system $F_0(N,V,T)$ can be computed from

$$F_0(N,V,T) = F_{\rm E}(N,V,T) + \Delta F(N,V,T). \tag{7}$$

The nonequilibrium thermodynamic integration of the equilibrated Cu films and bulks was carried out in a canonical (NVT) ensemble at the investigated temperatures using LAMMPS packages. The fixed center-of-mass correction was applied in the simulations. The switching time $t_{\rm s}$ is 5×10^5 timesteps in either the forward or backward Frenkel–Ladd switching process. Before switching, the system was equilibrated for 10^5 timesteps. Three independent Frenkel–Ladd procedures were performed to evaluate the statistical errors.

3. Results

Figure 2 illustrates a typical radial distribution function of the films with different atomic layers at 200 K. The first peaks of thin films perform left shifts, indicating that the average atomic spacings shrink with the decrease in film thickness, as demonstrated in Fig. 2(a). When the films are thick enough, the positions of the first peaks in the radial distribution functions are relatively fixed, as illustrated in Fig. 2(b). Figure 3(a) shows that the surface areas of the films contract as the thickness of the films decreases, which is consistent with the variations of the radial distribution function. The size effects become increasingly prominent, especially as the films are thinner than a critical value ($\sim$ 6 nm). This signifies that surface areas are rather sensitive to the thickness of the films. The thickness effects on the surface area are similar to the size effects on many physical and chemical properties, such as the melting temperature, the critical ferromagnetic, ferroelectric, superconductive transition temperature of nanocrystals, the glass formation ability, the Debye temperature, and the volume thermal expansion coefficient.[3,39–41] The surface contraction is always ascribed to the tensile surface stress originating from the electron redistribution and attractive interactions between surface atoms.[21] It is regarded that the surface atoms with one side exposed in the vacuum receive less constraints from other atoms compared to the bulk atoms inside the films. Thus, the surface atoms have a lower electron density compared to the bulk atoms. To increase the local electron density, surface atoms tend to adopt a smaller equilibrium spacing than the bulk. To increase the local electron density up to the extent of bulk atoms, surface atoms locate in a smaller interatomic spacing distances than bulk atoms, which is directly demonstrated by the contraction of the atomic layer spacing in the x or y direction, as illustrated in Fig. 3(b).

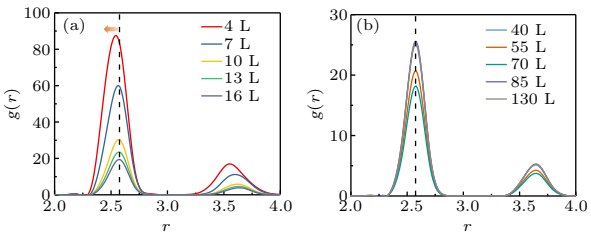


Fig. 2. The radial distribution functions of the films with different atomic layers at 200 K.

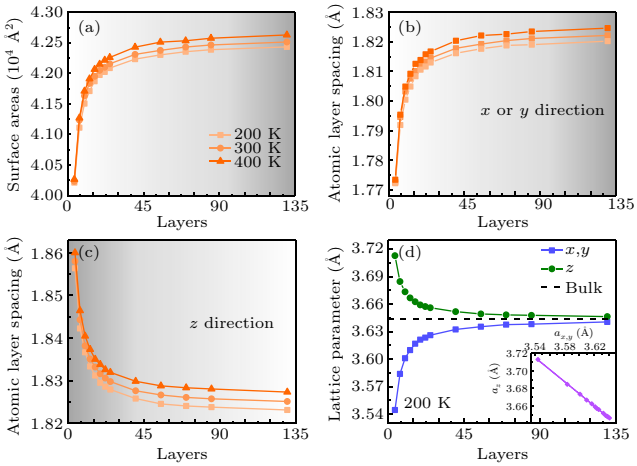


Fig. 3. The surface area of the films (a), the atomic layer spacing in the x or y axis (b) and z axis (c), and the lattice parameter of the films at 200 K (d) as a function of the thickness of the films. The inset in (d) displays the linear relationship between lattice parameters along the x/y axis and the z axis.

In terms of metallic bulks, metallic bonds usually lack strong directionality. As a result, it is always regarded that lattice contraction is isotropic with the decrease in material sizes. To test this speculation, we calculate the averaged atomic layer spacing along the z axis as $a_z = TH/(n-1)$, where n represents the number of atomic layers of the films, and TH is the different value of the averaged z coordinates of the top and bottom atoms in the films, as shown in Fig. 1(c). Remarkably, the atomic layer spacings along the z axis expand with decreasing film thicknesses, as shown in Fig. 3(c), which is totally opposite to those along the x or y axis in Fig. 3(b). The atomic layer spacing is half of the lattice parameter in this work. We show the variations of lattice parameters, for example at 200 K, along the x/y and z axis in Fig. 3(d). It is obvious that the lattice parameters of the films in three directions approach each other and that of the bulk when the thickness of the films is $\sim$ 24 nm (130 atomic layers). This indicates that the size effects of surfaces are very small then. The linear relationship with a negative slope between lattice parameters along different directions in the inset of Fig. 3(d) signifies a synchronous size effect of the surface along the directions that are parallel and perpendicular to the surface. Evidently, the exposed surfaces cause lattice distortion in the Cu films. The structure of Cu evolves from cubic to tetragonal with decreasing film thicknesses. Lattice contractions along the x/y axis ($\sim$ 2.71%

of ~ 0.5 nm film compared to bulks at 200 K, which is comparable to the experimental results[17]) is more severe than the lattice expansions along the z axis ($\sim 1.90\%$) in the same conditions. Consequently, it is considered that the competing behavior in two directions causes the inconsistent lattice variations (averaged values in three directions) of nanoparticles measured by x-ray or electron diffraction in experiments: common contractions and occasion expansions. The morphology and specific surface area of the examined nanoparticles in experiments have a great impact on the lattice variations. If surface atoms of a nanoparticle with a certain morphology play a more dominant role than bulk atoms, the averaged lattice contraction of the whole would be observed in experiments and vice versa. The existence of the surfaces greatly affects isotropic metallic bonds. The cubic lattice changes to tetragonal. Thinner films exhibit lattice distortions more obviously, as demonstrated by the dramatically increasing barrier of lattice parameters in two directions with decreasing film thicknesses in Fig. 3(d).

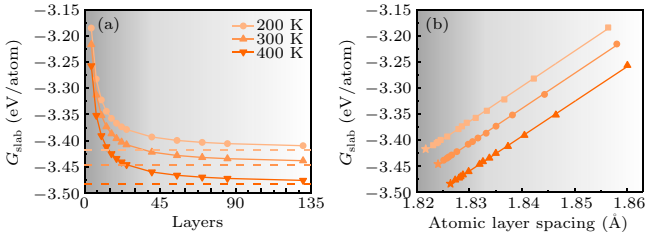


Fig. 4. The free energy of the films as a function of (a) the thicknesses of the films, and (b) the atomic layer spacing along the z axis. The dashed lines in (a) and the stars in (b) denote the free energy of the bulks at the corresponding temperatures.

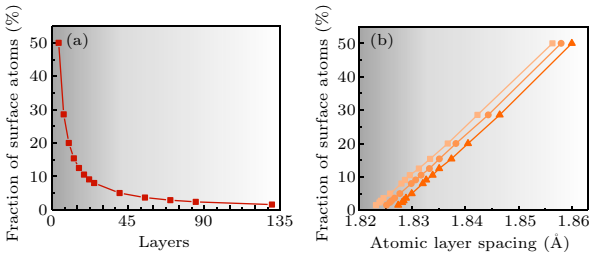


Fig. 5. The fraction of the number of surface atoms in the total atoms of the Cu films as a function of (a) the thicknesses of the films, and (b) the atomic layer spacing along the z axis.

To understand the thermodynamic essence of lattice distortions, we calculated the free energy and surface free energy of the films with different thicknesses. The thickness dependence of the free energy of the films is displayed in Fig. 4(a). The free energy of the films increases together with the decrease in the thickness and the climbs apparently accelerate, especially when the films are thinner than ~ 6 nm. According to the thermodynamic rule that the solid with lower energy is more stable,[42] thin films are less stable than thick films. Interestingly, the free energy of the films is linearly correlated with the atomic layer spacing, as shown in Fig. 4(b), indicating a direct relationship between lattice distortions and free energy. The existence of surface atoms is a critical factor for the variations of lattice parameters and energy. We thus evaluate the fraction of the surface atoms in the films. It emerges that the number of surface atoms accounts for increasingly larger fractions in the films with decreasing thicknesses, as shown in Fig. 5(a), which is consistent with the variations of lattice parameters in Fig. 3 and of the free energy in Fig. 4. Moreover, the fraction of the surface atoms is linearly correlated with the atomic layer spacing in accordance with the variations of free energy in Fig. 4(b). Consequently, it is clear why surface atomic layers play a critical role in the size effects on prevalent physical and chemical properties, and the influence of the surface improves dramatically as the thickness of the films decreases.

The exposed surface atoms have excess free energy compared to the atoms in bulks. Based on the obtained free energy of the films and bulks, the surface free energy per unit area of the films is then calculated as $\gamma = N_{\text{film}}(G_{\text{film}} - G_{\text{bulk}})/2A_{\text{film}}$, where N_{film}, A_{film}, G_{film}, G_{bulk} represent the atomic number, the surface area, and the free energy per atom of the film as well as the free energy per atom of the bulk, respectively. The thickness dependent surface free energy per unit area of films is illustrated in Figs. 6(a) and 6(b), which is comparable to the results obtained using another EAM potential.[43] The surface free energy per unit area exhibits a variation tendency that is coincident with that of the free energy accompanied by increasing remarkable size effects with decreasing film thicknesses. From the perspective of thermodynamic rules, it can be concluded that the surfaces of thin films are much more active than those of thick films. This is a reasonable explanation for higher productivity and better catalytic activities of thinner Cu (100) films in experiments as well as stronger size effects of thinner film on these physical and chemical properties.[8] More importantly, there is a linear relationship between the surface free energy per unit area of films and the atomic layer spacing along the z axis with a positive slope and along the x/y axis with a negative slope. Thus, it is reasonable to infer that prevalent physical and chemical properties of films, such as the melting temperature, and the critical ferromagnetic and ferroelectric properties, are also linearly correlated with the lattice parameter as the size dependence of these physical and chemical properties is consistent with that of the surface free energy per unit area.[3,39–41] Our findings thus provide a crucial theoretical basis for predicting the properties of films with different thicknesses.

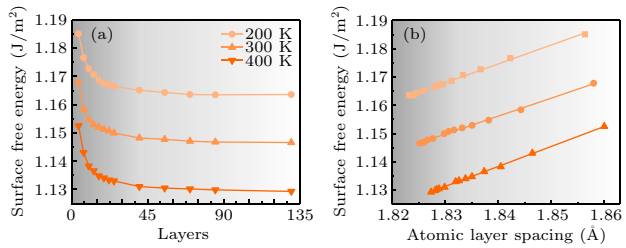


Fig. 6. The surface free energy per unit area of films as a function of (a) the thickness of the films, and (b) the atomic layer spacing along the z axis.

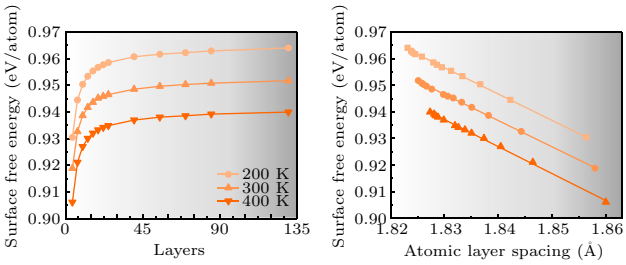


Fig. 7. The surface free energy per surface atom of films as a function of (a) the thickness of the films, and (b) the atomic layer spacing along the z axis.

In addition, we analyze the surface free energy in terms of per surface atom, which reflects the average excess free energy contributed by every surface atom. The surface free energy per surface atom is calculated as $\gamma = N_{\text{film}}(G_{\text{film}} - G_{\text{bulk}})/2N_{\text{surf}}$, where N_{surf} is the number of surface atoms on one side. Interestingly, the surface free energy per surface atom illustrated in Fig. 7(a) decreases with decreasing atomic layers, exhibiting an opposite trend to the surface free energy per unit area. Analogously, the surface free energy per surface atom is linearly related to the atomic layer spacing, as shown in Fig. 7(b). Referring to the variation of the surface areas in Fig. 3(a), the direct reason for the opposition between the surface free energy per unit area and the surface free energy per surface atom is that the surface area per surface atom reduces with decreasing film thickness. In fact, the controllable experimental parameter is not the number of surface atoms but always the surface area. Therefore, the important perspective responsible for the experimental research is that the surface free energy per unit area increases with the decrease in the thickness of the films.

4. Conclusion

In summary, size-dependent lattice contractions along the x/y axis and expansions along the z axis with decreasing thicknesses are observed in clean Cu (100) films using molecular dynamics simulations. The physical origin of lattice variations could be attributed to the increasing surface free energy per unit area with decreasing film thicknesses. It is worth noting that the surface stresses exert non-negligible effects on the internal atoms of the films, which cause the lattice expansion along the z axis of the films. The competing mechanism of stresses parallel and perpendicular to the surface should be responsible for the inconsistent lattice variations of nanoparticles observed in previous experimental investigations. The morphology and specific surface area of the nanoparticles have a great impact on the lattice variations. It is expected that there could be a critical size of Cu nanoparticles dividing the lattice contraction and expansion. This is a promising topic for further studies, and we ask that more attention should be paid to the distinction of lattice variations along different directions, regardless of the films or of the nanoparticles, in more metallic systems in the future.

Acknowledgments

Project supported by the fellowship of China Postdoctoral Science Foundation (Grant No. 2021T140073), the National Natural Science Foundation of China (Grant No. 5210011290), the Science Challenge Project of China (Grant No. TZ2018002), and the National Key Research and Development Program of China (Grant No. 2016YFB0201204).

References

[1] Park N J, Field D P, Nowell M M and Besser P R 2005 *J. Electron. Mater.* **34** 1500
[2] Liu H D, Zhao Y P, Ramanath G, Murarka S P and Wang G C 2001 *Thin Solid Films* **384** 151
[3] Yang C C and Jiang Q 2005 *Acta Mater.* **53** 3305
[4] Jiang Q and Lu H M 2008 *Surf. Sci. Rep.* **63** 427
[5] Mistry H, Varela A S, Kühl S, Strasser P and Cuenya B R 2016 *Nat. Rev. Mater.* **1** 16009
[6] Muttaqien F, Hamamoto Y, Hamada I, Inagaki K, Shiozawa Y, Mukai K, Koitaya T, Yoshimoto S, Yoshinobu J and Morikawa Y 2017 *J. Chem. Phys.* **147** 094702
[7] Cheng T, Xiao H and Goddard W A 2017 *Proc. Natl. Acad. Sci. USA* **114** 1795
[8] Zhao J, Xue S, Barber J, Zhou Y, Meng J and Ke X 2020 *J. Mater. Chem. A* **8** 4700
[9] Reske R, Duca M, Oezaslan M, Schouten K J P, Koper M T M and Strasser P 2013 *J. Phys. Chem. Lett.* **4** 2410
[10] Mistry H, Reske R, Zeng Z, Zhao Z J, Greeley J, Strasser P and Cuenya B R 2014 *J. Am. Chem. Soc.* **136** 16473
[11] Back S, Yeom M S and Jung Y 2015 *ACS Catal.* **5** 5089
[12] Diehm P M, Áoston P and Albe K 2012 *ChemPhysChem* **13** 2443
[13] Nafday D, Sarkar S, Ayyub P and Saha-Dasgupta T 2018 *ACS Nano* **12** 7246
[14] Wang L, Zeng Z, Gao W, Maxson T, Raciti D, Giroux M, Pan X, Wang C and Greeley J 2019 *Science* **363** 870
[15] Sheng J, Welzel U and Mittemeijer E J 2010 *Appl. Phys. Lett.* **97** 153109
[16] Champion Y, Bernard F, Millot N and Perriat P 2005 *Appl. Phys. Lett.* **86** 231914
[17] Wasserman H J and Vermaak J S 1972 *Surf. Sci.* **32** 168
[18] Birringer R, Hoffmann M and Zimmer P 2002 *Phys. Rev. Lett.* **88** 206104
[19] Apai G, Hamilton J F, Stohr J and Thompson A 1979 *Phys. Rev. Lett.* **43** 165
[20] Liu X D, Zhang H Y, Lu K and Hu Z Q 1994 *J. Phys.: Condens. Matter* **6** L497
[21] Cammarata R C and Sieradzki K 1994 *Annu. Rev. Mater. Sci.* **24** 215
[22] Jamshidian M, Thamburaja P and Rabczuk T 2015 *Phys. Chem. Chem. Phys.* **17** 25494
[23] Bonzel H P and Nowicki M 2004 *Phys. Rev. B* **70** 245430
[24] Abbasian A, Ghaffarian S R, Mohammadi N and Fallahi D 2004 *J. Appl. Polym. Sci.* **93** 1972
[25] Aragones J L, Valeriani C and Vega C 2012 *J. Chem. Phys.* **137** 146101

[26] Rickman J M and LeSar R 2002 *Annu. Rev. Mater. Res.* **32** 195

[27] Frenkel D and Ladd A J C 1984 *J. Chem. Phys.* **81** 3188

[28] Frenkel D and Smith B 2002 *Understanding Molecular Simulation: From Algorithms to Applications* (Elsevier: Oxford)

[29] Allen M P and Tildesley D J 2017 *Computer Simulation of Liquids* (OUP Oxford: United Kingdom)

[30] Jarzynski C 2011 *Ann. Rev. Conden. Matter Phys.* **2** 329

[31] Jarzynski C 1997 *Phys. Rev. Lett.* **78** 2690

[32] Freitas R, Asta M and de Koning M 2016 *Comp. Mater. Sci.* **112** 333

[33] Paula Leite R and de Koning M 2019 *Comp. Mater. Sci.* **159** 316

[34] Plimpton S 1995 *J. Comput. Phys.* **117** 1

[35] Mendelev M I, Rahman M J, Hoyt J J and Asta M 2010 *Modell. Simul. Mater. Sci. Eng.* **18** 074002

[36] Trong D N, Long V C and Ţălu Ş 2022 *Appl. Sci.* **12** 4437

[37] Zou L, Yang C, Lei Y, Zakharov D, Wiezorek J M K, Su D, Yin Q, Li J, Liu Z, Stach E A, Yang J C, Qi L, Wang G and Zhou G 2018 *Nat. Mater.* **17** 56

[38] Mendelev M I, Kramer M J, Becker C A and Asta M 2008 *Philos. Mag.* **88** 1723

[39] Joshi N, Mathur N, Mane T and Sundaram D 2018 *Comp. Mater. Sci.* **145** 140

[40] Yang C C and Li S 2007 *Phys. Rev. B* **75** 165413

[41] An S, Su R, Zhao S, Liu J, Liu B and Guan P 2018 *Phys. Rev. B* **98** 134101

[42] Pelton A D M K H, Kurz W, Brener E, Murch G E, Binder K, Wagner R, Kampmann R, Voorhees P W, Binder K, Fratzl P, Purdy G R, Bréchet Y J M, Inden G, Delaey L and Kunz M 2001 *Phase transformations in materials* (Weinheim: Wiley)

[43] Gumbsch P and Daw M S 1991 *Phys. Rev. B* **44** 3934